

# Kinetics of titanium silicide formation on single-crystal Si: Experiment and modeling

C. A. Pico and M. G. Lagally

Materials Science Program, University of Wisconsin at Madison, Madison, Wisconsin 53706

(Received 21 March 1988; accepted for publication 21 July 1988)

The growth kinetics of titanium silicide grown from thin-film Ti-on-Si(100) and Si(111) reaction couples are investigated using primarily Auger electron spectroscopy. A Ti/precursor-phase/TiSi<sub>2</sub>/Si layered structure is found. The growth law of TiSi<sub>2</sub> depends on substrate orientation. An activation enthalpy of  $\Delta H = 2.5\text{--}2.6 \pm 0.25$  eV/atom, substantially higher than previously reported values, is determined. The total silicide growth (TiSi<sub>2</sub> + precursor) has nearly a parabolic time dependence implying that the precursor phase forms as " $At^{1/2} - Bt$ " using Si(111) as a substrate. A model based on mass diffusion from a moving interface is presented and is shown to be in good agreement with the experimental results. This model, which is used to determine the diffusion coefficient of Si in the precursor phase, can be applied to other similar binary compound systems containing line compounds.

## I. INTRODUCTION

Refractory-metal silicides are currently receiving widespread attention because of their usefulness as interconnects in very large scale integrated (VLSI) devices.<sup>1-5</sup> Presently the prime candidate is TiSi<sub>2</sub> grown from Ti-on-Si reaction couples because of its low resistivity and relatively low processing temperature.<sup>6</sup> One key problem that faces the immediate use of TiSi<sub>2</sub> is reproducibility during growth. This has been reflected in the wide variation of results published in the literature on TiSi<sub>2</sub> and its related compounds. An understanding of the fundamental mechanisms involved in the formation of TiSi<sub>2</sub> is necessary if it is to be used effectively in VLSI devices.

Experimental evidence for TiSi<sub>2</sub> grown from Ti-on-Si reaction couples initially led to the conclusion that TiSi<sub>2</sub> formation is diffusion limited ( $\alpha t^{1/2}$ ) with an activation energy of  $\Delta H = 1.8$  eV/atom. This conclusion was based on observed changes during sample annealing of the measured sheet resistance,<sup>7</sup> on x-ray diffraction (XRD) profiles,<sup>7</sup> on investigations of lateral silicide growth,<sup>8</sup> consumed Si,<sup>7,9</sup> phase thickness,<sup>10</sup> and dopant concentration profiles.<sup>11</sup> However, all but direct measurement of phase thicknesses can be shown to be misleading in their conclusions. For example, the identification of TiSi detected by XRD<sup>7,12</sup> can be reinterpreted (and necessarily so) as being TiSi<sub>2</sub> (C49).<sup>13</sup> Of the studies using observed phase thickness measurements, different experiments have shown evidence of differing growth kinetics,<sup>11,14,15</sup> but have been interpreted on the basis of the initial conclusions above.

In order to determine unambiguously the kinetics of titanium silicide formation, we have performed a process-consistent study of the properties of TiSi<sub>2</sub> grown from Ti-on-Si reaction couples by systematically varying individual process parameters such as substrate surface orientation, film thickness, annealing temperature, and annealing time. We report here the results of our investigations of the kinetics of formation of TiSi<sub>2</sub> and its related precursor phase (presum-

ably TiSi) as a function of the orientation of single-crystal substrates. Although previous studies of the kinetics of TiSi<sub>2</sub> formation have been made for a variety of substrates, each has used only one type of substrate. We determine the kinetics of formation of both TiSi<sub>2</sub> and the total silicide on Si(100) and Si(111) substrates for anneal temperatures between 470 and 650 °C. Using these results we develop a model of phase growth from a moving interface and extract the diffusion coefficient of Si in the phase that forms prior to TiSi<sub>2</sub> (precursor phase) and determine the activation enthalpy for formation of this precursor phase. Possible mechanisms of titanium silicide phase formation are presented and discussed. Lastly, we compare our results with those previously published and account for their differences.

## II. EXPERIMENT

Commercially prepared and polished, lightly doped ( $\sim 10$  Ω cm) *p*-type Si(100) and Si(111) single-crystal substrates were organically cleaned (acetone, methanol) before being chemically cleaned (three cycles of HNO<sub>3</sub>, HF, deionized water rinse). The substrates were immediately placed in reagent-grade methanol to minimize reoxidation during the transfer from the chemical cleaning area to the deposition chamber. The substrates were loaded moist with methanol in the cryo- and turbopumped vacuum system. The deposition chamber was then pumped down to  $10^{-6}$  Torr within 3-4 min. Ultimate background pressure varied from 4 to  $9 \times 10^{-8}$  Torr during the course of experiments and was achieved after simultaneous cryo- and turbopumping for  $\sim 4$  h.

Thin (700-3000 Å) films of Ti were electron-beam (*e*-beam) evaporated onto the single-crystal Si substrates. Prior to deposition, Ti was evaporated onto a closed shutter to clean the source material and to provide additional getter pumping during evaporation. Ti was then evaporated onto the substrates at 20 Å/s using a quartz crystal microbalance as the monitor. Early during Ti deposition the background

pressure rose to  $2 \times 10^{-7}$  Torr, presumably from  $H_2O$  outgassing from the surrounding shielding. In some cases, the pressure had reached  $\sim 1 \times 10^{-6}$  Torr towards the end of deposition. This could be avoided by allowing the Ti source and shielding to cool to room temperature prior to deposition. With this procedure the background pressure never rose above  $1.0 \times 10^{-7}$  Torr during deposition.

After deposition the wafers were removed from the deposition chamber, cleaved ( $0.3 \text{ cm} \times 0.3 \text{ cm}$ ), and encapsulated with a Ti getter in small (diameter = 1 cm, length = 5 cm) quartz ampoules evacuated under  $2 \times 10^{-6}$  Torr vacuum for subsequent annealing. At  $2 \times 10^{-6}$  Torr, the encapsulated background gas is equivalent to less than a monolayer of impurities on the sample (which has already been exposed to air). The getter was independently heated prior to annealing to provide an internal pumping surface for background contaminants. The samples were annealed at  $470\text{--}650^\circ\text{C}$  in a tube furnace for times ranging from 20 min to several hours. Anneal times were considered to begin 2–4 min after inserting the sample into the tube furnace. During this time the furnace temperature recovered to nearly its intended value. It was controlled thereafter to within  $1^\circ\text{C}$ .

Reaction couples of  $3000\text{-}\text{\AA}$  Ti-on-Si(111) and Si(100) were then analyzed to determine silicide phase presence and the kinetics of silicide phase formation. The Ti thickness of  $3000 \text{ \AA}$  was chosen to minimize the influence of the outer surface during this study while still providing the local properties associated with thin films during silicide formation. To determine if phase formation is related to film thickness, growth using  $700\text{-}\text{\AA}$  and  $2000\text{-}\text{\AA}$  layers of Ti-on-Si(111) was compared to that for  $3000\text{-}\text{\AA}$  layers of Ti.

Detection and characterization of phases present in partially and fully reacted Ti-on-Si reaction couples were done using Auger electron spectroscopy (AES) depth profiling,  $\Theta\text{-}2\Theta$  and Read camera XRD, and transmission electron microscopy (TEM). AES depth profiling was used to obtain elemental composition as a function of depth into the annealed samples. The AES results were complemented by separate x-ray photoelectron spectroscopy (XPS) and Rutherford backscattering (RBS) measurements. In all cases the location of the interface between two phases was chosen to be at the midpoint (i.e., average) of Ti signal intensity between plateaus associated with these phases.  $\Theta\text{-}2\Theta$  XRD was used to determine quantitatively the crystallography and the relative crystal orientations in the films. Read camera XRD was used to detect crystallographic phases in films where phases are too thin to be detected by  $\Theta\text{-}2\Theta$  XRD. TEM was used to determine the microstructures and crystallographies in the films. By correlating the results of these measurements it is possible to substantiate conclusions reached on each individual set of our measurements.

### III. RESULTS

#### A. Compositional analysis and phase growth

AES analysis of as-deposited Ti films showed  $< 1\text{--}2\%$  O and C impurities in the bulk. Near the outer surface (within  $\sim 300 \text{ \AA}$ ) O levels rose monotonically to up to  $\sim 5\%$ . There was no evidence of impurities at the Ti/Si interface. Partially annealed reaction couples showed a Ti/precursor/TiSi<sub>2</sub>/Si layered structure (Fig. 1) for both Si substrate orientations regardless of original Ti film thickness. The precursor and TiSi<sub>2</sub> phase grew as long as a Ti overlayer existed. After the Ti overlayer was exhausted (except the last  $\sim 100\text{--}300 \text{ \AA}$ ), the growth of the TiSi<sub>2</sub> phase continued unperturbed until all of the precursor phase was consumed; at this point TiSi<sub>2</sub> formation ceased and the film remained constant in composition. Although silicide formation was detected at  $470^\circ\text{C}$ , the TiSi<sub>2</sub> phase could not be compositionally distinguished below  $500^\circ\text{C}$ . The unreacted Ti film remaining in partially reacted samples contained up to  $15\%$  O and  $\sim 2\%$  C. The total integrated O in this remaining Ti film was much higher than in the as-deposited sample, indicating that most of the O contamination is introduced (presumably from  $H_2O$  absorbed on the encapsulant walls) during the anneal step. C levels dropped off monotonically with depth into the sample. This contamination did not appear to inhibit any further silicide formation except that the last  $\sim 100\text{--}300 \text{ \AA}$  of Ti generally did not react to form silicide but remained as impure Ti—probably a mixture of oxide, carbide, and Ti. The C and O impurities were detected in trace amounts ( $< 2\%$ ) in the precursor phase and were below detection limits ( $< 0.5\%$ ) in the TiSi<sub>2</sub> layer. No impurities were detected at or below the TiSi<sub>2</sub>/Si interface. No other impurities were detected besides C and O.

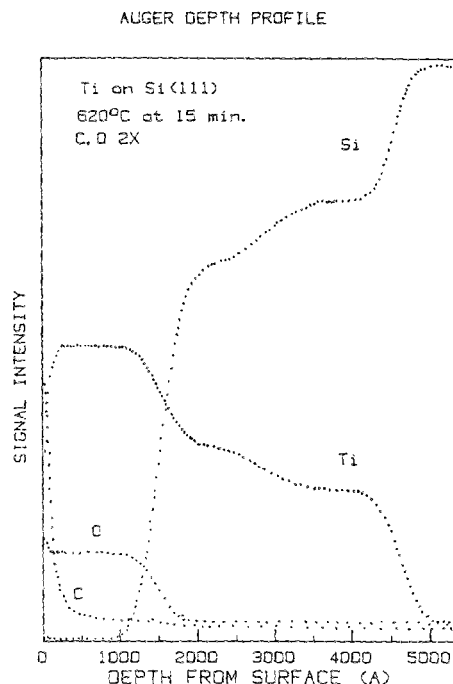


FIG. 1. Typical AES depth concentration profile of a partially reacted  $3000\text{-}\text{\AA}$  Ti-on-Si reaction couple. Contamination levels are below detection limits in the region near the precursor-phase/TiSi<sub>2</sub> interface.

After the Ti overlayer was exhausted (except the last  $\sim 100\text{--}300 \text{ \AA}$ ), the growth of the TiSi<sub>2</sub> phase continued unperturbed until all of the precursor phase was consumed; at this point TiSi<sub>2</sub> formation ceased and the film remained constant in composition. Although silicide formation was detected at  $470^\circ\text{C}$ , the TiSi<sub>2</sub> phase could not be compositionally distinguished below  $500^\circ\text{C}$ . The unreacted Ti film remaining in partially reacted samples contained up to  $15\%$  O and  $\sim 2\%$  C. The total integrated O in this remaining Ti film was much higher than in the as-deposited sample, indicating that most of the O contamination is introduced (presumably from  $H_2O$  absorbed on the encapsulant walls) during the anneal step. C levels dropped off monotonically with depth into the sample. This contamination did not appear to inhibit any further silicide formation except that the last  $\sim 100\text{--}300 \text{ \AA}$  of Ti generally did not react to form silicide but remained as impure Ti—probably a mixture of oxide, carbide, and Ti. The C and O impurities were detected in trace amounts ( $< 2\%$ ) in the precursor phase and were below detection limits ( $< 0.5\%$ ) in the TiSi<sub>2</sub> layer. No impurities were detected at or below the TiSi<sub>2</sub>/Si interface. No other impurities were detected besides C and O.

Absolute Si/Ti ratios using AES depth profiling could not be made with high accuracy because of uncertain Si and Ti sensitivity factors and preferential sputtering. The composition of the TiSi<sub>2</sub> phase was determined by comparing the AES data to those of fully reacted films in which the XRD and resistivity were characteristic of TiSi<sub>2</sub>. Subsequent XPS

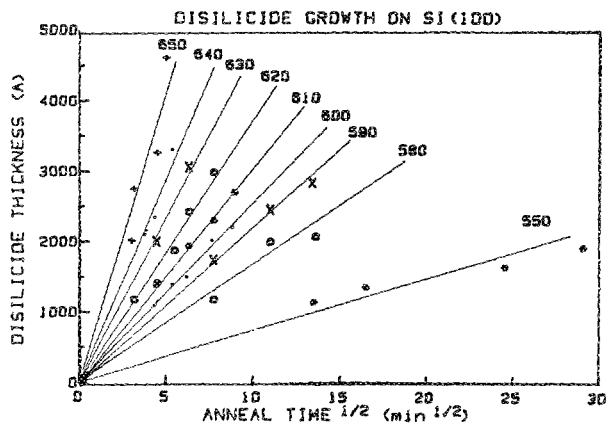


FIG. 2. Dependence of the  $\text{TiSi}_2$  thickness grown on Si(100) substrates for various anneal temperatures on the square root of time.

and RBS depth profiling analysis of partially reacted 3000- and 700-Å Ti-on-Si(111) reaction couples, respectively, confirmed the Ti/precursor/ $\text{TiSi}_2$ /Si layered structure. The precursor phase has a Si/Ti composition ratio of  $\sim 1$ .

The rate of growth of  $\text{TiSi}_2$  from 3000-Å-thick Ti-on-Si(100) and Si(111) reaction couples as a function of annealing temperature was measured using AES depth profiling.  $\text{TiSi}_2$  formed parabolically with time ( $\alpha t^{1/2}$ ) on Si(100) (Fig. 2) with a diffusional activation enthalpy (Fig. 3) of  $\Delta H = 2.5 \pm 0.25$  eV. On Si(111)  $\text{TiSi}_2$  formed linearly with time ( $\alpha t$ ) (Fig. 4). The activation enthalpy depth profiling

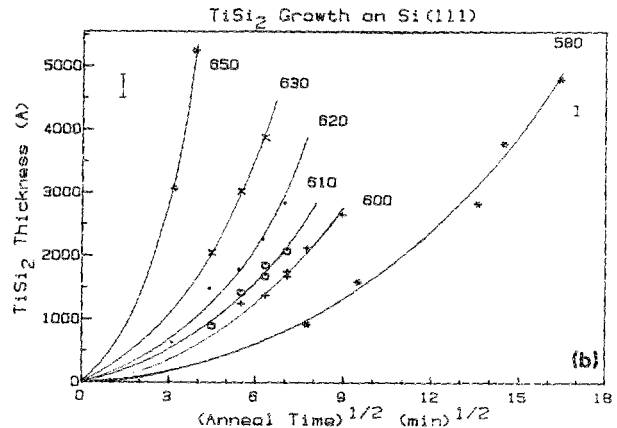
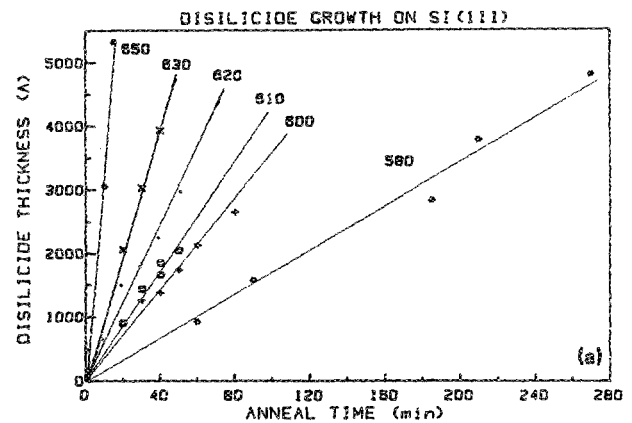


FIG. 4. Dependence of the  $\text{TiSi}_2$  thickness grown on Si(111) substrates for various anneal temperatures on (a) time and (b) the square root of time. The plot shows that a straight line fit can be obtained only for a linear time dependence and not for a parabolic one.

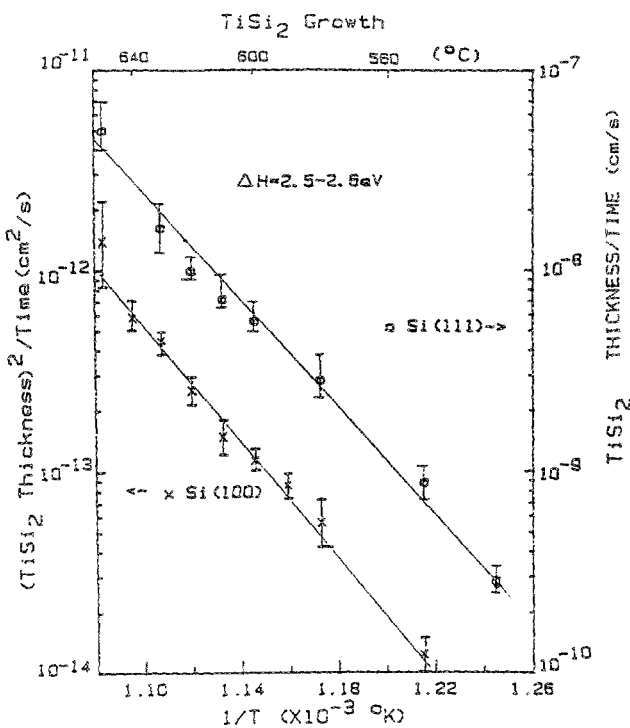


FIG. 3. Arrhenius plot of the change of the square of the  $\text{TiSi}_2$  thickness with anneal time on Si(100) (left) and the growth rate of  $\text{TiSi}_2$  on Si(111) (right).

anneals of, respectively, 200- and 700-Å Ti-on-Si(111) gave the same linear  $\text{TiSi}_2$  growth as their 3000-Å counterpart.

From the same AES depth profiles the rate of growth of the total silicide thickness (precursor +  $\text{TiSi}_2$ ) [this must not be confused with "total number of reacted Si atoms" (see discussion below)] was extracted as a function of temperature. The increase in total silicide thickness can be fit with a curve following a  $t^{1/2}$  behavior using Si(100) substrates and nearly as  $t^{1/2}$  on Si(111) (Fig. 5). An Arrhenius plot (Fig. 6) of the data for both Si orientations gives a single straight line from which a diffusional activation enthalpy of  $\Delta H = 2.6 \pm 0.25$  eV can be extracted.

### B. Crystallographic and microstructural analysis

$\Theta$ - $2\Theta$  XRD showed the presence of Ti and  $\text{TiSi}_2$  in partially reacted films when phase thicknesses were over 1000 Å. Silicide diffraction intensity peaks were found at higher-than-predicted angles indicating a compressive strain parallel to the Si substrate of 1%–3%.  $\text{TiSi}$  detection and determination of the  $\text{TiSi}_2$  structure (C49 or C54) were not possible because of these high strains. Relative peak intensities for each phase were constant on each substrate throughout anneals. In fully annealed samples having resistivities characteristic of C54 (11–14  $\mu\Omega$  cm), it was found that the

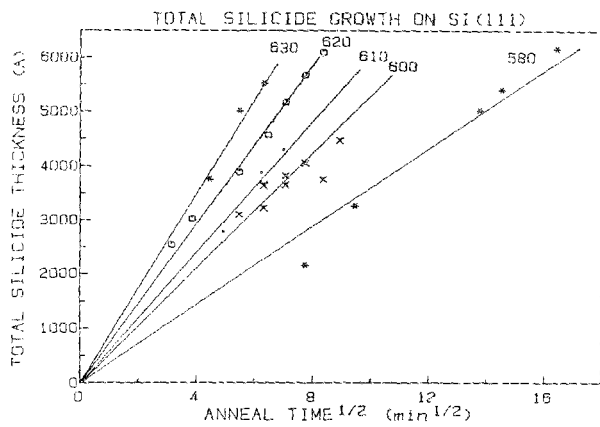


FIG. 5. Dependence of the total silicide thickness grown on Si(111) substrates on the square root of time for various anneal temperatures.

crystallographic orientation of  $\text{TiSi}_2$  changes with Si substrate orientation (Fig. 7). Read Camera XRD detected many more diffraction peaks than had been seen previously with  $\Theta$ - $2\Theta$  XRD. However, peak-position determination using Read camera XRD is much less accurate than that of  $\Theta$ - $2\Theta$  XRD. Unfortunately, no unambiguous diffraction peaks indicating the presence of  $\text{TiSi}$ ,  $\text{Ti}_5\text{Si}_4$ , or  $\text{Ti}_5\text{Si}_3$  could be determined under any condition, even when using  $1\text{-}\mu\text{m}$ -thick films of Ti.

No definitive conclusion could be drawn concerning Ti/precursor/ $\text{TiSi}_2$ /Si layered structure by cross-sectional TEM. While columnar grains of  $\text{TiSi}_2$  were readily detected,

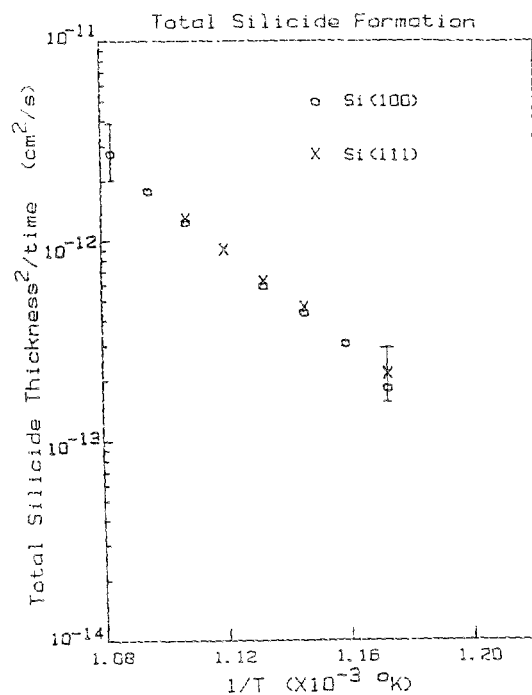


FIG. 6. Arrhenius plot of the change of the square of the total silicide thickness with anneal time on Si(100) and Si(111) substrates. The activation enthalpy is  $\Delta H = 2.6 \pm 0.25$  eV/atom.

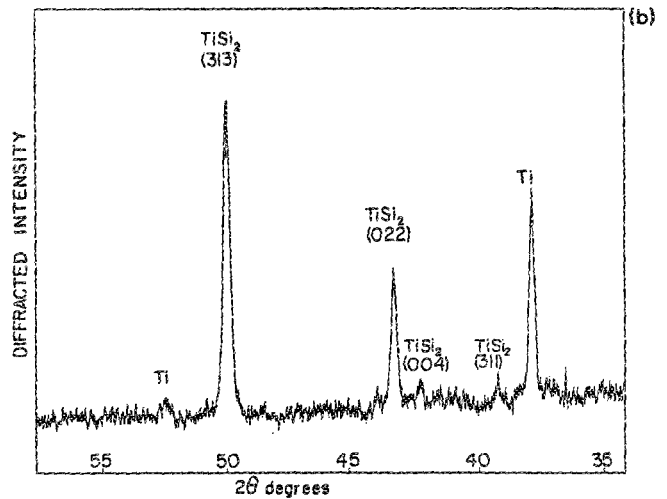
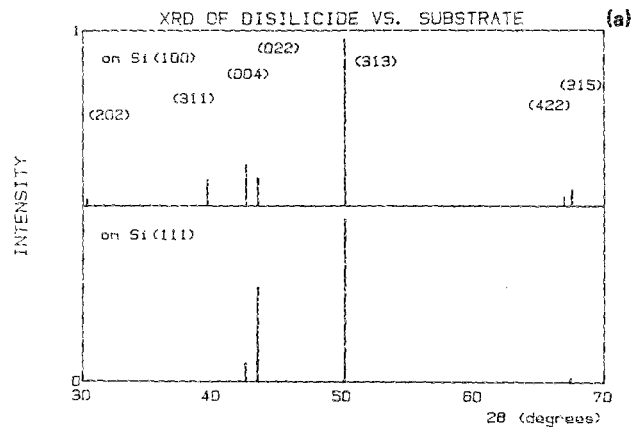


FIG. 7. Schematic diagrams of XRD  $\Theta$ - $2\Theta$  profiles (a) of  $\text{TiSi}_2$  grown from a 17-min anneal at  $700^\circ\text{C}$  of  $1\text{-}\mu\text{m}$  Ti-on-Si(100) (above) and Si(111) (below). Observed  $\text{TiSi}_2$  (C54) crystalline orientations are shown in parentheses above peaks. The plots are normalized at the (313) peak. An example of an experimental XRD  $\Theta$ - $2\Theta$  profile is shown in (b) for reference. [Note that the angular scale runs in a direction opposite to (a)].

$\text{TiSi}$  or any other phase could not be detected using micromicrodiffraction. The  $\text{TiSi}_2$ /Si interfacial roughness was of the order of  $200 \text{ \AA}$ . No impurities were detected in the films by energy-dispersive x-ray spectroscopy (EDS), although elements with  $Z$  numbers less than that of Na are not detectable because of a Be window between the sample and the EDS detector. It was determined by microdiffraction that the  $\text{TiSi}_2$  had a C49 structure in films partially annealed at and below  $630^\circ\text{C}$ . No samples were investigated by TEM for higher annealing temperatures; however, we have determined, using resistivity measurements,<sup>16</sup> that C49 ( $55\text{--}65 \mu\Omega \text{ cm}$ ) transforms into C54 near  $630^\circ\text{C}$  after some nucleation time.

#### IV. DISCUSSION

##### A. $\text{TiSi}_2$ , precursor-phase, and total-silicide growth kinetics

It was determined that the growth of  $\text{TiSi}_2$  from Ti-on-Si reaction couples depends on the orientation of the Si sub-

strate.  $\text{TiSi}_2$  grows parabolically with time ( $\alpha t^{1/2}$ ) on Si(100) with an activation enthalpy of  $\Delta H = 2.6 \pm 0.25$  eV/atom and linearly with time ( $\alpha t$ ) on Si(111) with an activation enthalpy of  $\Delta H = 2.5 \pm 0.25$  eV/atom. (Note: the slight change in the reported value of  $\Delta H$  of  $\text{TiSi}_2$  formation from that in Ref. 17 is a result of a statistical analysis of the actual data points, as opposed to an average of the limits set by the error bars.) As a consequence, the thickness of  $\text{TiSi}_2$  grown for a given anneal time and temperature varies on different substrate orientations. An example is shown in Fig. 8, which shows that the  $\text{TiSi}_2$  thickness on Si(100) is initially greater at short anneal times but then becomes less than that on Si(111) at longer anneal times at the same temperature.

It has been believed that the kinetics of  $\text{TiSi}_2$  formation is diffusion limited with an activation enthalpy for diffusion of  $\Delta H = 1.8$  eV/atom regardless of Si substrate conditions. Any variation from this behavior was considered as an artifact of impurities introduced unintentionally.<sup>15,16</sup> Because the other processing parameters in our experiments were identical, differences in growth kinetics of  $\text{TiSi}_2$  within our experiments must be due to substrate orientation. If film contamination were the cause of the different types of kinetics, one would not expect to see the behavior exhibited in Fig. 8 and still have both types of samples exhibit the same enthalpy of formation.

The total-silicide thickness (precursor +  $\text{TiSi}_2$ ) was determined to grow nearly parabolically with time regardless of  $\text{TiSi}_2$  growth kinetics. Furthermore, when plotted on an Arrhenius plot, the (total-silicide thickness)<sup>2</sup>/(anneal time) data on both Si(100) and Si(111) substrates lie on the same straight line with an activation enthalpy of  $\Delta H = 2.6 \pm 0.25$  eV. These results imply that the precursor phase grows nearly as " $At^{1/2} - Bt$ " on Si(111).

In the Appendix we develop a diffusional model accounting for the growth of the precursor phase in reaction couples that exhibit parabolic or linear  $\text{TiSi}_2$  growth kinetics. Our model predicts that the precursor phase should form as  $At^{1/2}$  when  $\text{TiSi}_2$  grows parabolically with time and as

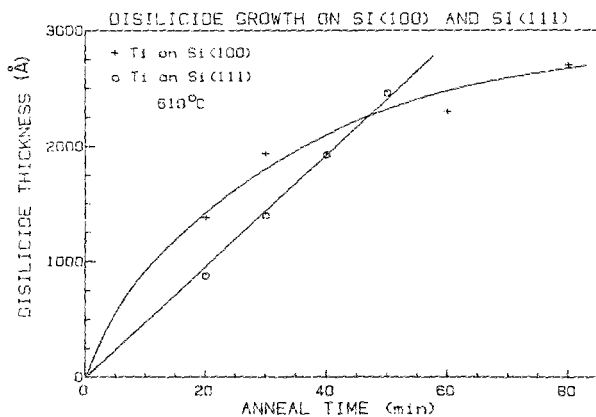


FIG. 8. Comparison of  $\text{TiSi}_2$  formed from Ti-on-Si(100) and Si(111) under identical annealing (610°C) conditions. The thickness is plotted vs anneal time. Note that the disilicide initially grows faster on Si(100) than on Si(111), but subsequently grows more slowly.

" $At^{1/2} - Bt$ " (plus higher-order terms) when  $\text{TiSi}_2$  grows linearly with time. Furthermore, we have determined that other models, such as those with a  $\log(t)$  growth or more simplified models, could not be fit to agree with our data. Using our model it is possible to extract the diffusion coefficient of Si in the precursor phase as a function of temperature. These values are plotted from 550 to 650 K in Fig. 9. They lie on a straight line with an activation enthalpy of  $\Delta H = 2.5 \pm 0.25$  eV/atom.

## B. Possible mechanisms for $\text{TiSi}_2$ formation

While the formation of  $\text{TiSi}_2$  on Si(100) is readily explained by diffusion-controlled growth, the reasons for its linear growth on Si(111) remain to be determined. The presence of a diffusion or reaction barrier at either the Si/ $\text{TiSi}_2$  or the  $\text{TiSi}_2$ /precursor-phase interface could cause linear growth of  $\text{TiSi}_2$ .

Because the activation enthalpies for  $\text{TiSi}_2$  formation, total-silicide thickness growth, and precursor-phase formation are so similar, we look for models based on dominant diffusion-type mechanisms located at the precursor phase/ $\text{TiSi}_2$  interface that will explain the linear growth of  $\text{TiSi}_2$  and would allow an additional diffusional flux of Si into the precursor phase. We discuss four possible mechanisms for this linear growth and decide whether there is any evidence of their occurrence. The four mechanisms are:

(a) A barrier at the precursor-phase/ $\text{TiSi}_2$  interface could be caused by a reaction between the diffusing Si and

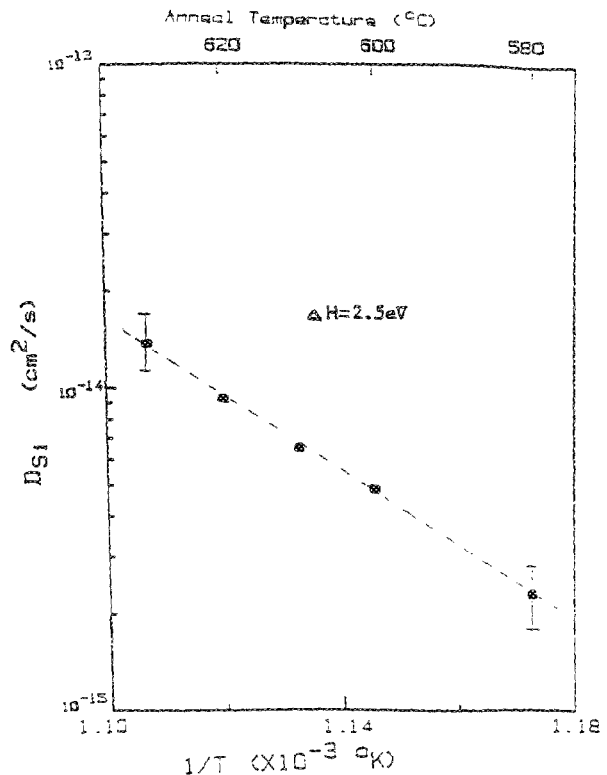


FIG. 9. Arrhenius plot of the diffusion coefficient of Si in the precursor phase (presumably  $\text{TiSi}$ ) formed from anneals of Ti-on-Si(111). Diffusion coefficients were extracted by the method described in the Appendix.

precursor-phase matrix. If there is a barrier at the interface related to specific site reactions, such as layer-by-layer (Frank-van der Merwe) growth in which a new layer will not nucleate until the previous layer is completed, the growth will be limited by the movement of atoms near this interface to the specific locations where they can react. In this case, the growth will be linear with an activation enthalpy nearly identical to that of bulk diffusion. The growth rate will be significantly less than that obtained through diffusion control. Possible evidence for site specificity is seen in TEM investigations of the C49 phase in which long-range ( $2\ \mu\text{m}$ ) grain and faulting orientation occurs. However, because the linear growth rates on Si(111) are similar to those of the parabolic growth on Si(100), it is unlikely that this is the mechanism responsible for the linear growth.

(b) A diffusion barrier at the precursor-phase/TiSi<sub>2</sub> interface could be induced by stress. This would be manifested in a potential gradient affecting diffusion. A potential gradient,  $-F$ , would change the concentration flux at any point,  $x$ , so that

$$J = -D \left( \frac{dc}{dx} \right) - cv, \quad (1)$$

in one dimension, where  $v = B/F$  and  $B = D/kT$  is the mobility of Si. The solution to Fick's second law for a constant planar source at  $x = 0$  is then

$$c = A \{ 1 - \text{erf}[(x - vt + \Delta)/(4Dt)^{1/2}] \}, \quad (2)$$

where  $A$  is the normalization constant and  $\Delta$  is a constant determined by the boundary conditions. This implies that the concentration remains constant throughout time at  $x = vt - \Delta$ . Such a condition would satisfy the constant velocity precursor-phase/TiSi<sub>2</sub> interface and our observations that the activation enthalpy for TiSi<sub>2</sub> growth on Si(111) is the same as the diffusion coefficient determined from Si(111). Furthermore, this would be consistent with our model for the precursor-phase formation in which the Si concentration is assumed constant at the precursor-phase/TiSi<sub>2</sub> interface. However, silicide-phase growth consistent with concentration flux and concentration requires several additional complicated assumptions (e.g., a strain layer that maintains a concentration equilibrium with both the matrix and the interface) for the model to work.

(c) Growth involving film cracking can lead to linear time dependence. This model originates from corrosion-oxidation studies<sup>19</sup> and is as follows: As Si diffuses into the region near the precursor-phase/TiSi<sub>2</sub> interface, strain builds to high amounts. At some point small fissures induced by this strain form, creating fresh surfaces for the Si to diffuse into. If this happens repeatedly, the growth of the TiSi<sub>2</sub> phase will be governed by a superposition of diffusional interfaces and it follows that TiSi<sub>2</sub> growth will be (on the average) linear with time. This process is assisted by the fact that, once started, cracks propagate linearly with time. Because the velocity of the precursor-phase/TiSi<sub>2</sub> interface is linearly dependent on  $D$ , the activation enthalpy will be identical to that of diffusion. If this mechanism is the cause of linear growth we would expect to see remnants of cracking and concentration variations in the TiSi<sub>2</sub> on a microscopic level on those substrates that exhibit linear growth kinetics [i.e.,

on Si(111)]. While TEM investigations show that TiSi<sub>2</sub> has a high concentration of planar defects (with interplanar distance of 30–100 Å) when formed on Si(111), compositional analysis using a  $< 5\text{-\AA}$  probe across these defects showed no variation of composition. Furthermore, this faulting has also been seen when formed on Si(100)<sup>20</sup> where TiSi<sub>2</sub> formation is parabolic in time. From these observations we conclude that linear growth caused by film cracking does not account for the linear growth kinetics of TiSi<sub>2</sub>.

(d) Another possible barrier is related to the movement of dislocations at the precursor-phase/TiSi<sub>2</sub> interface. It has been shown that the TiSi<sub>2</sub>/Si interface is semicoherent.<sup>13</sup> If the precursor phase is crystalline, it would not be surprising if the precursor-phase/TiSi<sub>2</sub> interface is also semicoherent. Strains incurred by changes in the crystal structures at the interface are alleviated by transformation dislocations at this interface. Growth of this phase would be limited by diffusion-assisted movement (glide followed by climb) of these transformation dislocations.<sup>21</sup> It has been shown for elemental materials<sup>22</sup> that a dislocation,  $b$ , in bulk material under stress climbs at a velocity

$$v = 2\pi D_s \sigma b_s v_a / b_e^2 kT \ln(R/b), \quad (3)$$

where  $D_s$  is the self-diffusion coefficient,  $\sigma$  is the stress in the neighborhood of the dislocation,  $b_e$  and  $b_s$  are the edge and screw components of the dislocation,  $v_a$  is the atomic volume,  $T$  is the temperature, and  $R$  is the radius of the strain field. While this expression is meant to describe elemental materials, it should apply nearly as well to compound materials containing a primary diffusant (in our case, Si). For the precursor-phase/TiSi<sub>2</sub> interface, Eq. (3) can then be interpreted as the movement of transformation dislocations<sup>21</sup> in the precursor phase. Because the dislocation climb depends on  $D_s$ , the activation enthalpy of TiSi<sub>2</sub> formation (i.e., dislocation climb) will be identical to that of the precursor phase. We find that the growth rates predicted from Eq. (3) are extremely close to experimentally determined values of  $v$ . For example, at 600 °C available values for  $D_{\text{Si}} = 4.9 \times 10^{-15} \text{ cm}^2/\text{s}$  (Fig. 9),  $\sigma \sim 10^3 \text{ J/cm}^3$ ,<sup>7</sup>  $b_e \sim 3.4 \text{ \AA}$  (lattice spacing for nearest Ti–Ti bond in C49),  $b_s \sim 0.5 \text{ \AA}$  (arbitrarily chosen), and  $R/b \sim 10^4$  (Ref. 22) give a predicted TiSi/TiSi<sub>2</sub> interface velocity of 1 Å/s. This value is close to our measured value of 3 Å/s. In addition to TiSi<sub>2</sub>-phase growth by dislocation climb, diffusant can continue unhindered through the interface between dislocations. Regular growth of the precursor phase would then continue via diffusion-limited growth from a moving interface. The growth rate would be similar to that of diffusional growth and thus fit within the restrictions of experimental observations. While the dislocation climb model is the most plausible of the four considered, confirmation of the experiments<sup>23,24</sup> indicating that the precursor phase is highly disordered would show that it is not possible.

### C. Comparison of kinetics of silicide growth with previous investigations

Since no previous study has reported linear growth, comparison of our titanium silicide growth results to those of others is limited to studies in which parabolic growth was

observed. Because a comparable study on Si(100) used "total number of reacted Si atoms" as the unit of measurement,<sup>15</sup> we have replotted our data and that of Revesz and co-workers<sup>11</sup> in this way on an Arrhenius plot (Fig. 10) against their data for comparison. While the activation enthalpy extracted from these plots have been used to determine the kinetics of silicide formation, they are only averages over the film thickness. The results of the study done by Hung *et al.*<sup>10</sup> using *a*-Si substrates have been included, even though they are not directly comparable, because their data have, essentially, been the standard for comparison. (It is interesting to note that our investigations on low-pressure CVD *a*-Si gave a linear TiSi<sub>2</sub> growth with a similar activation enthalpy as reported here.<sup>25</sup>) Other published data were not included because they are impossible to compare consistently.

We find that the data in Refs. 8 and 15 lie below but parallel to ours, implying the same activation enthalpy. Residual impurities could easily lower the data without changing the activation enthalpy as long as the concentrations of extrinsic defects (i.e., impurities) are significantly below those of intrinsic defects (vacancies, etc.). In general, the higher the preexponential factor, the more representative the data are of a clean system. We therefore believe that our data are more reliable than those lying on parallel lines below our plots.

The data by Hung *et al.*<sup>10</sup> which represent only TiSi<sub>2</sub>

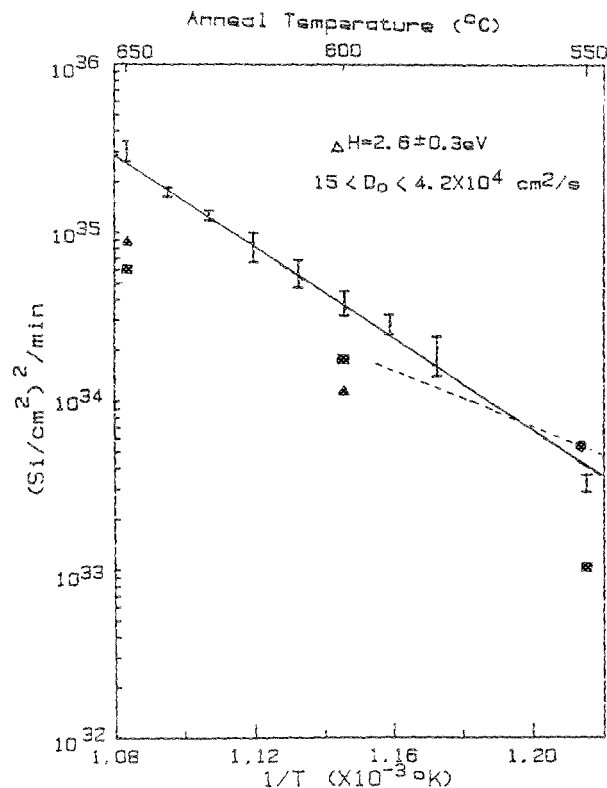


FIG. 10. Arrhenius plot of the (number of reacted Si atoms)<sup>2</sup>/time as reported here (error bars), by Hung *et al.*<sup>10</sup> (dot), Revesz, Gyimesi, and Zsoldos<sup>11</sup> (triangles), and Bentini *et al.*<sup>15</sup> (squares). The dashed line represents an extrapolation of the data in Ref. 10.

(no other phase existed) lie on a line having a lesser slope than that of our data, and crosses at  $\sim 550$  K. Had we included only TiSi<sub>2</sub> in our analysis, the line representing our data would be lower but would retain the same slope. Reference 10 reports an activation enthalpy of  $\Delta H = 1.8$  eV/atom. Although strain can affect the diffusion coefficient, the magnitude of observed strain ( $< 3\%$ ) has an insignificant effect on it. It is more likely that the difference between our measured activation enthalpies and those of Ref. 10 is related to film impurities. It is clear how the preexponential factor can be influenced by impurities, e.g., by blocking some possible hopping sites. But a significant presence of impurities in the film could cause a change from intrinsic to extrinsic diffusion and would, ultimately, define the rate at which Si could diffuse into the overlying film to form more silicide. In intrinsic materials the vacancy concentration is an entropy-driven process, whereas in extrinsic materials vacancy concentration is defined by the type and number of impurities. Because diffusion is a two-step process (vacancy formation followed by atom migration), the activation enthalpy that one measures in intrinsic diffusion will be the sum of that of vacancy formation and that of atomic migration. While the latter does not change significantly with impurity content, the contribution of vacancy formation to the enthalpy of diffusion disappears in extrinsic materials. Hence, a higher activation enthalpy implies a "cleaner" film. The preexponential diffusion coefficient in extrinsic diffusion is several orders of magnitude less than that of intrinsic diffusion because the possible substitutional paths are "tied up" or "plugged up" by impurities (except for extrinsic vacancies). When compared to those previously reported, our observed activation enthalpies are  $\sim 0.8$  eV/atom higher (approximately the energy necessary for the creation of vacancies<sup>26</sup>) and our preexponential diffusion coefficients are substantially higher imply our results represent the Ti-on-Si reaction couple more accurately.

To demonstrate that impurities have affected many kinetics studies, one needs only to look at the other experiments that have deduced a value of  $\Delta H \sim 1.8$ – $2.0$  eV/atom. The appearance and disappearance of other silicide phases in these studies suggests the presence of impurities.<sup>10,14,15</sup> One of the key experiments that helps confirm the conclusion that  $\Delta H \sim 1.8$  eV/atom is the investigation of the diffusive behavior of implanted dopants.<sup>11,26</sup> In one experiment<sup>11</sup> the implanted dopant, Sb, diffused upon annealing with an activation enthalpy of  $\Delta H = 1.9$  eV/atom. Recently, a similar study was done<sup>27</sup> using this and other dopants, with the identical conclusion with one exception. The exception occurred when Ge was used as the implanted dopant. In this case the activation enthalpy was notably higher than 2 eV/atom. Because Ge has a valence state similar to that of Si, it is expected that the behavior of Ge in a Ti environment will be similar to that of Si. It is, therefore, expected that Ge will not deplete intrinsic vacancies in the same manner that other impurities, e.g., P, would. Similar arguments can be made in the classic experiments by Murarka and Fraser<sup>7</sup> using heavily P-doped poly-Si substrates.

The conclusion that impurities are responsible for the lower activation enthalpies previously observed is also con-

sistent with experimental technique, in which the primary difference is annealing ambients. Most comparable experiments use a vacuum ( $5 \times 10^{-7}$  Torr) furnace while we use vacuum encapsulation. In a vacuum furnace the ambient around the sample is constantly refreshed. We speculate that nitrogen (the primary component of air), which has the same valence as P and forms Ti compounds, is introduced during these anneals and induces extrinsic diffusion when no other impurities were deliberately added. From the above discussion, we conclude that  $\Delta H_p = 0.8$  eV/atom for vacancy formation and  $\Delta H_m = 1.8$  eV/atom for atomic migration.

## V. SUMMARY

We have investigated the growth of the silicide phases formed from anneals of thin-film Ti-on-Si reaction couples. We have found that a Ti/precursor-phase/TiSi<sub>2</sub>/Si layered structure occurs. We have shown that TiSi<sub>2</sub> grows linearly with time ( $\alpha t$ ) on Si(111) and parabolically with time ( $\alpha t^{1/2}$ ) on Si(100). We have also shown that the growth of the total-silicide thickness is nearly parabolic with time regardless of substrate orientation. We show through a mathematical model that this behavior of growth of the total silicide is expected if a reaction or diffusion barrier exists at the TiSi<sub>2</sub>/precursor-phase interface. Using this model we have determined the diffusion coefficient of Si in the precursor phase as a function of temperature. In all cases, the activation enthalpy of silicide formation or Si diffusion is  $\Delta H = 2.5$ – $2.6$  eV/atom. This value is substantially higher than those previously published and we attribute this to fewer reactive impurities in our films.

## ACKNOWLEDGMENTS

This research was sponsored by the Semiconductor Research Corporation under Contract No. SRC 083-01-027. We thank D. Coulman, Hewlett-Packard Research Laboratories, Palo Alto, CA, for the RBS data and N. Tran, University of Wisconsin-Madison, Madison, WI, for the XPS data. We thank P. Shewman, Ohio State University, Columbus, OH, for reviewing the Appendix. We thank D. Aaron, R. Cooper, D. Savage, and R. Thomas for useful discussions.

## APPENDIX

Growth of two intermediate phases in a reaction couple when diffusion limits the rate of growth can be solved analytically. However, it is not clear how to determine the growth characteristics when the kinetics of phase formation are different (e.g., reaction and diffusion) for each phase. It appears to be solvable only by numerical methods.<sup>28</sup> Still, it is helpful to obtain an approximate analytical solution to model the growth of phases in these cases.

Below we develop a generalized theoretical model of intermediate phase formation from a diffusional reaction couple involving a moving planar source that can be applied to the growth of neighboring phases having different mechanisms controlling their growth. This model is applied to phase formation when the location of the planar source is determined by diffusional ( $\alpha t^{1/2}$ ) and interfacial reaction

( $\alpha t$ ) kinetics. For the latter we provide a direct expression for determining the diffusion coefficient without the previously necessary measurement of the absolute diffusant concentration within the growing phase. This expression is valuable for systems containing line compounds whose composition changes less than 1% within the phase and cannot be measured otherwise.

## A. Previous theories of layered phase formation

Two different mechanisms are responsible for layered phase formation: diffusion and interfacial reaction. In thin-film reaction couples these mechanisms are, in general, characterized by a parabolic and linear time dependence. There have been many different approaches<sup>29,30</sup> to model the growth of a single intermediate phase in which both of its interfaces are characterized by the same type of growth kinetics. These models arrive at the same mathematical description as that of Deal and Grove.<sup>31</sup> The rate of growth of an intermediate phase is given by

$$\frac{dx}{dt} = \frac{G\Delta Ck}{(1 + kx/D)}, \quad (\text{A1})$$

where  $G$  is a constant determined by the relative phase compositions at each interface,  $k$  is the reaction constant,  $\Delta C$  is the change in the concentration within the growing phase, and  $D$  is the diffusion coefficient (assuming one diffusing species) in the material. This model gives a linear growth rate at short times and parabolic growth at longer times. Any quantitative growth information using Eq. (A1) requires an accurate knowledge of  $\Delta C$ . This is extremely difficult if not impossible in line compounds. It follows that the Deal and Grove model is primarily useful for and limited to providing a qualitative understanding of intermediate phase growth.

In systems having more than one phase and dominated by diffusional kinetics, the concentration profile maintains its error function dependence on distance/ $t^{1/2}$  as described for single-phase growth in general textbooks, although the expression becomes more complex.<sup>32</sup> Kidson<sup>33</sup> has derived a generalized expression for the width of any given phase in a diffusional reaction couple. This is given by

$$x_{i-1,i} = 2[(DK)_{i-1,i} - (DK)_{i,i-1}/c_{i-1,i} - c_{i,i-1}](t)^{1/2}, \quad (\text{A2})$$

where  $c_{i,i-1}$  is the concentration of the diffusing species and  $D_{i,i-1}$  is the diffusion constant of the diffusing species at the  $X_{i-1}/X_i$  interface and  $x_{i-1,i}$  is the thickness of phase  $i$  and

$$K_{i,i-1} = (t)^{1/2} \left( \frac{dc}{dx} \right)_{i,i-1}. \quad (\text{A3})$$

Because of the parabolic time dependence of the interfacial position,  $K_{i,i-1}$  is a constant. It follows that the interfaces described in Eq. (A2) move parabolically with time. However, the diffusion coefficients in line compounds cannot be determined.

## B. Model of phase formation having a moving planar diffusant source

The physical situation we will treat is a three-phase reaction couple (1/2/3) in which material 1 diffuses into phases 2 and 3. We then extrapolate this to a four-phase reaction

couple by assuming that the total amount of diffusant that enters phase 3 does not diffuse into phase 4 but provides only interfacial reaction material. Phase 1 is the source material. The mathematical origin is chosen at the phase-1/phase-2 interface. The position of the phase-2/phase-3 interface is given as  $f(t)$ . Phase-3 growth is dictated by the diffusion of material 1 from this moving interface into phase 3. To find an approximate solution, three assumptions are made.

- (1) Only one diffusing species.
- (2) The growth rate of phase 3 is determined by the concentration of the diffusing species at the phase-2/phase-3 interface.
- (3) The concentration of the diffusant is at saturation at this interface.

The first assumption is for simplicity and is representative of the experimental observation that Si diffuses roughly ten times faster than Ti. The second is an assumption of a boundary value problem. The last corresponds to a situation in which the diffusion in phase 2 is faster than in phase 3 and in which the diffusant solubility is higher in phase 2.

Physically, we have pictured a planar diffusion source at the phase-2/phase-3 interface. To solve the time dependence of phase-3 growth we need to consider the Green's function satisfying the one-dimensional diffusion equation. This is, in generalized form,<sup>32</sup>

$$c(x, x', t, t') = [A(x', t, t') / (t - t')^{1/2}] \times \exp[-(x - x')^2 / 4D(t - t')] \quad (\text{A4})$$

where  $(x', t')$  is the space-time coordinate of the planar source at the phase-2/phase-3 interface and  $A(x', t, t')$  is its normalization factor. The expression for  $A(x', t, t')$  is determined by normalization or by comparison with a known solution. The total concentration of diffusant is then the superposition of the sources

$$c(x, t) = \sum_x \sum_{t'} c(x, x', t, t') = \int dx' \int dt' c(x, x', t, t'). \quad (\text{A5})$$

In a boundary-value problem one of the primed coordinates can be eliminated. Choosing the distribution at  $t' = 0$ , the concentration is expressed as

$$c(x, t) = \int dx' \frac{A(x', t)}{t^{1/2}} \exp\left(\frac{-(x - x')^2}{4Dt}\right). \quad (\text{A6})$$

By fixing the source at  $x' = 0$  (i.e., phase-2/phase-3 interface), the concentration is expressed as

$$c(x, t) = \int dt' \frac{A(t, t')}{(t - t')^{1/2}} \exp\left(\frac{-x^2}{4D(t - t')}\right). \quad (\text{A7})$$

In either case, the total diffused amount of the diffusant across the phase-2/phase-3 interface,  $M$ , to the right (positive  $x$  axis) of a plane at  $x$  is

$$M = \int_x^\infty c(x, t) dx. \quad (\text{A8})$$

Determination of the growth of phase 3 for the case when the concentration has a fixed value,  $c_0$ , at the phase-2/phase-3 interface ( $x' = 0$ ) can be achieved using either Eqs. (A6) or (A7). The former equation can be forced to meet the boundary condition by assuming (for convenience,

we let the minimum concentration in phase 3 be defined as zero)

$$c(x' < 0, t = 0) = c_0, \quad (\text{A9})$$

$$c(x' > 0, t = 0) = 0.$$

(Note that the condition to the left of  $x = 0$  is physically artificial.) The solution to Eq. (A6) is

$$c(x, t) = A' \{1 - B \operatorname{erf}[x / (4Dt)^{1/2}]\}, \quad (\text{A10})$$

in phase 3 and it follows that the phase grows as

$$M = Ct^{1/2}. \quad (\text{A11})$$

Obtaining these results using Eq. (A7) requires a known  $A(t, t')$ . By matching the concentration at  $x = 0$  and  $dc/dx$  everywhere, we find

$$A(t, t') = A'' / t^{1/2}. \quad (\text{A12})$$

This means, in order to force the concentration at  $x = 0$  to be constant, the planar source must "release" atoms with a frequency proportional to the square root of time. Physically, this corresponds to a decreasing localized diffusant concentration near the interface caused by a local saturation by the diffusing species. The solution to the concentration profile is then the same as Eq. (A10). For Eq. (A12) to hold for a moving interface, it must be that the concentration at the interface does not change with time. This, however, is one of our three initial assumptions.

Applying this analysis to a moving interface whose position is described as

$$x' = f(t'), \quad (\text{A13})$$

we assume that  $A(t, t')$  has the same functional form. This assumption meets the requirement that the concentration at  $x' = f(t')$  is  $c_0$ . The growth of material to the right of  $x'$  at some time  $t$  is

$$M = \int_0^t dt' \int_{f(t')}^\infty dx \{a / [t(t - t')]^{1/2}\} \times \exp\{-[x - f(t')]^2 / 4D(t - t')\}. \quad (\text{A14})$$

By integration over  $x$ , Eq. (A14) becomes

$$M = b(4D/t)^{1/2} \int t' dt' \times \{1 - \operatorname{erf}[x - f(t') / [4D(t - t')]^{1/2}]\}, \quad (\text{A15})$$

where  $b$  is a constant and

$$\operatorname{erf}(x) = 2(\pi)^{-1/2} \int_0^x \exp(u^2) du, \quad (\text{A16})$$

is tabulated elsewhere.<sup>31</sup> A generalized analytical solution of Eq. (A15) is not possible. However, by Taylor series expanding the exponential in the error function and integrating term by term, the total diffused mass to the right of  $x = f(t)$  is

$$M = b \left(\frac{4D}{t}\right)^{1/2} \int_0^t dt' \times \left[1 - \left(u - \frac{u^3}{3} + \frac{u^5}{10} - \frac{u^7}{42} \pm \dots\right)\right], \quad (\text{A17})$$

where

$$u = [x - f(t') / [4D(t - t')]^{1/2}] \quad (\text{A18})$$

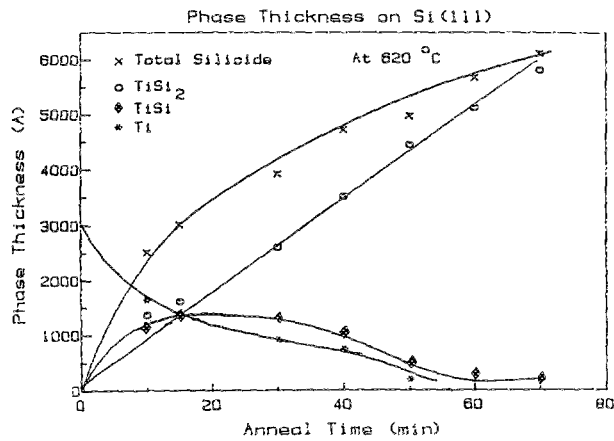


FIG. 11. Thicknesses of the various phases formed from 620 °C anneals of Ti-on-Si(111) as a function of anneal time.

is a dimensionless number.

Two cases are of specific interest. The first is that in which the phase-2/phase-3 interface moves as defined by diffusion (i.e.,  $\sim t^{1/2}$ ). In this case,

$$f(t') = At'^{1/2}, \quad (\text{A19})$$

and the solution for mass flux is

$$M = A(c_3, D_2, D_3)t^{1/2}, \quad (\text{A20})$$

where  $A(c_3, D_2, D_3)$  is a constant depending on the diffusant concentration,  $c_3$ , and diffusion coefficients of phase 2 and phase 3,  $D_2$  and  $D_3$ , respectively. The second case of interest is that which has the interface moving linearly with time (i.e.,  $x' = vt$ ). The solution to the total diffused mass is

$$M = A(D_3) [t^{1/2} - \frac{2}{3}at + \frac{2}{15}a^3t^2 \pm \dots], \quad (\text{A21})$$

where

$$a = v/(4D_3)^{1/2}. \quad (\text{A22})$$

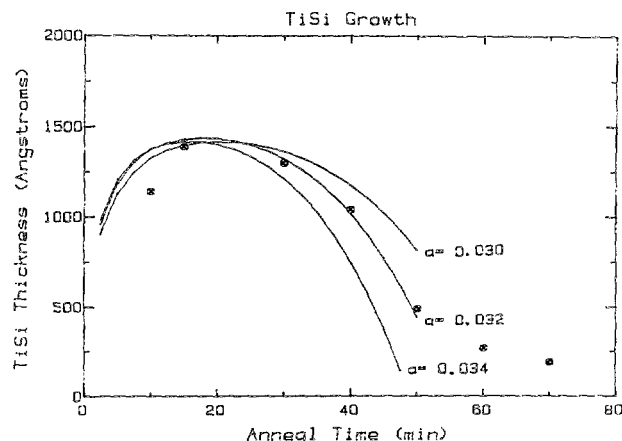


FIG. 12. Comparison of the measured (dots) precursor-phase (presumably TiSi) thickness as a function of anneal time with theoretical fit (lines). This procedure is used for extracting  $D_{Si}$  in the precursor phase. The parameter "a" is given by  $v/\sqrt{4D_{Si}}$ .

At this point numerical evaluation is needed to determine which terms in Eq. (A21) are significant. This model has one adjustable parameter, "a", that depends solely on the value of the diffusion coefficient of Si in the precursor phase. This adjustable parameter can be uniquely determined by fitting the predicted curve with that of the measured growth of the precursor phase. In Fig. 11 we have plotted the measured thicknesses of the various phases that occur in the Ti-on-Si(111) reaction couple formed from 620 °C anneals. Correspondingly, we have plotted in Fig. 12 the predicted behavior against our experimental results for the growth of the precursor phase formed from 620 °C anneals on Si(111). While the value of "a" is chosen by the best fit to the curve, we see that the fit is extremely sensitive to small (5%) variations of "a" when all but the first five terms are included (an estimated error of  $\sim 20\%$  is possible). Agreement between model and experiment is good for anneal times up to 50 min. Sometime after 50 min, the Ti overlayer is consumed and the growth of the precursor phase changes and no longer follows the growth predicted by Eq. (A21). Similar agreement occurs at other anneal temperatures. In this way we have extracted the diffusion coefficients for Si in the precursor phase growing on Si(111) substrates.

One consequence of our model of precursor-phase growth is that it allows one to extract the real diffusion coefficient of the precursor phase even if the concentration profile of Si is not known. This is, to our knowledge, the first treatment in which a calculation independent of concentration profiles can reveal the diffusion coefficient of a diffusant.

- <sup>1</sup>S. P. Murarka, *Silicides for VLSI Applications* (Academic, New York, 1983).
- <sup>2</sup>K. N. Tu and J. W. Mayer, in *Thin Films-Interfaces and Reactions*, edited by J. M. Poate, K. N. Tu, and J. W. Mayer (Wiley, New York, 1978), Chap. 10.
- <sup>3</sup>G. Ottaviani, *J. Vac. Sci. Technol.* **16**, 1112 (1979).
- <sup>4</sup>S. P. Murarka, *J. Vac. Sci. Technol.* **17**, 775 (1980).
- <sup>5</sup>S. P. Murarka, M. H. Read, C. J. Doherty, and D. B. Fraser, *J. Electrochem. Soc.* **129**, 293 (1982).
- <sup>6</sup>C. Y. Ting, S. S. Iyer, C. M. Osburn, G. J. Hu, and A. M. Schweighart, *VLSI Science and Technology*, edited by C. J. Dell'Oca and W. M. Bullis (The Electrochemistry Society, 1982), p. 224.
- <sup>7</sup>S. P. Murarka and D. B. Fraser, *J. Appl. Phys.* **51**, 342 (1980).
- <sup>8</sup>P. Revesz, J. Gyimesi, L. Pogany, and G. Peto, *J. Appl. Phys.* **54**, 2114 (1983).
- <sup>9</sup>A. Guldán, V. Schiller, A. Steffen, and P. Balk, *Thin Solid Films* **100**, 1 (1983).
- <sup>10</sup>L. S. Hung, J. Gyulai, J. W. Mayer, S. S. Lau, and M. A. Nicolet, *J. Appl. Phys.* **54**, 5076 (1983).
- <sup>11</sup>P. Revesz, J. Gyimesi, and E. Zsoldos, *J. Appl. Phys.* **54**, 1860 (1983).
- <sup>12</sup>E. Zsoldos, G. Peto, V. Schiller, and G. Valyi, *Thin Solid Films* **137**, 243 (1986).
- <sup>13</sup>R. Beyers and R. Sinclair, *J. Appl. Phys.* **57**, 5240 (1985).
- <sup>14</sup>J. S. Maa, C. J. Lin, J. H. Liu, and Y. C. Liu, *Thin Solid Films* **64**, 439 (1979).
- <sup>15</sup>G. G. Bentini, R. Nipoti, A. Armigliato, M. Berti, A. V. Drigo, and C. Cohen, *J. Appl. Phys.* **51**, 270 (1985).
- <sup>16</sup>C. A. Pico and M. G. Lagally (unpublished).
- <sup>17</sup>C. A. Pico, N. C. Tran, J. R. Jacobs, and M. G. Lagally, *Mater. Res. Soc. Proc.* **71**, 315 (1986).
- <sup>18</sup>T. G. Finstad and M. A. Nicolet, *Thin Solid Films* **68**, 393 (1980).
- <sup>19</sup>C. R. Barrett, W. D. Nix, and A. S. Tetelman, *The Principles of Engineering Materials* (Prentice Hall, Englewood Cliffs, NJ, 1973), Chap. 12.

- <sup>20</sup>T. C. Chou, C. Y. Wong, and K. N. Tu, *J. Appl. Phys.* **62**, 2275 (1987).
- <sup>21</sup>D. Cherns and D. A. Smith, *Defects in Semiconductors*, edited by Narayan and Tan (North-Holland, New York, 1981), p. 291.
- <sup>22</sup>J. P. Hirth and J. Lothe, *Theory of Dislocations* (Wiley, New York, 1982), Chap. 15.
- <sup>23</sup>K. Holloway and R. Sinclair, *J. Appl. Phys.* **61**, 1359 (1987).
- <sup>24</sup>J. C. Hensel, J. M. Vandenberg, F. C. Unterwald, and A. Maury, *Appl. Phys. Lett.* **51**, 1100 (1987).
- <sup>25</sup>C. A. Pico and M. G. Lagally (unpublished).
- <sup>26</sup>H. Schmalzried, *Solid State Reactions*, 2nd ed. (Chemie, Deerfield Beach, FL., 1981).
- <sup>27</sup>F. M. D'Heurle, A. E. Michel, F. K. LeGoues, G. Scilla, J. T. Wetzel, and P. Gas, *Mater. Res. Soc. Proc.* **77**, 333 (1987).
- <sup>28</sup>R. W. Balluffi and J. M. Blakely, *Thin Solid Film* **25**, 363 (1975).
- <sup>29</sup>F. Panini, M. Costato, and G. Majni, *Nuovo Cimento* **7D**, 241 (1986).
- <sup>30</sup>U. Gosele and K. N. Tu, *J. Appl. Phys.* **53**, 3252 (1982).
- <sup>31</sup>B. E. Deal and A. S. Grove, *J. Appl. Phys.* **36**, 3770 (1965).
- <sup>32</sup>J. Crank, *The Mathematics of Diffusion* (Oxford University Press, London, 1956).
- <sup>33</sup>G. V. Kidson, *J. Nucl. Mater.* **3**, 21 (1961).